

NUMERICAL AND EXPERIMENTAL ANALYSIS OF GROUTED HOLLOW BLOCK MASONRY UNDER COMPRESSION

Robertas Zavalis, Bronius Jonaitis, Gediminas Marčiukaitis

Vilnius Gediminas Technical University, Saulėtekio al. 11, LT-10223 Vilnius, Lithuania

Received 10 March 2013; accepted 31 May 2013

Abstract. Highly hollow masonry units, which allow reducing the weight of masonry constructions and improving heat and sound insulation qualities, are commonly used in masonry construction. Filling the hollows with concrete, or concrete with light additives, results in complex masonry. Overall performance of such masonry is affected by initial stresses, which are caused by shrinkage deformations of different infill concrete and masonry units. Behaviour of infill concrete and concrete blocks is analysed by applying numerical detailed micro modelling. Experiments revealed that masonry deformations of blocks with concrete filled hollows are similar to those of longitudinal deformations of infill concrete samples. σ - ε relations were received through numerical micro modelling and compressive strength of masonry match values were estimated during experiments.

Keywords: hollowness, concrete masonry units, concrete infill, shrinkage, numerical modelling.

Reference to this paper should be made as follows: Zavalis, R.; Jonaitis, B.; Marčiukaitis, G. 2013. Numerical and experimental analysis of grouted hollow block masonry under compression, *Engineering Structures and Technologies* 5(2): 45–53. <http://dx.doi.org/10.3846/2029882X.2013.811784>

Introduction. Stress state analysis of grouted block masonry

Highly hollow concrete masonry units are the most common in masonry construction. They help accelerating the construction process and reducing labour-related costs. Hollow masonry units decrease the natural weight of masonry constructions, improve physical properties of walls, such as noise and thermal insulation (Oan, Shive 2012). Occasionally, particular masonry construction elements, such as cavities between hatches and wall corner joints can be reinforced by filling in the hollowness, also, reinforced in-wall columns or ring beams can be installed. Hollow masonry units of a special construction solution can be used as a residual mould (Fig. 1). In such cases, monolith concrete or reinforced concrete walls are set.

To improve strength and stiffness of such block constructions, their hollowness is filled with concrete

(Fonseca, Siggard 2012). Block concrete and infill concrete have different properties. Blocks are made beforehand and their concrete structure is formed, concrete shrinkage deformations, which greatly influence concrete behaviour, have usually taken place. It is practically impossible to achieve such properties in hardened infill concrete poured into hollows. Acquired construction of the type consists of two layers, which

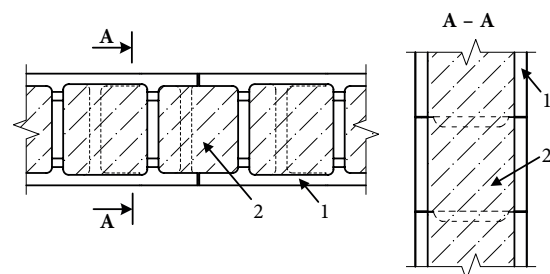


Fig. 1. Masonry unit with concrete filled hollowness masonry solution: 1 – hollow masonry unit; 2 – infill concrete

have different properties and their internal stress state changes upon start of infill concrete hardening (Fig. 2).

Assuming that infill concrete is not adhering to blocks, its deformations take place separately (Curve 4). Due to different deformation properties of the blocks and the infill concrete, the blocks are compressed and the infill concrete receives tensile stresses. If the surface of the blocks is humidified, concrete shrinkage deformations diminish (Curve 2). After pouring infill concrete, both elements (block and infill concrete) shrink in approximately the same way (Curves 3 and 5). Therefore, the difference between shrinkage deformations is significantly reduced, and adherence between the blocks and the infill concrete is improved. This is one of the main conditions for ensuring joint performance of both concrete layers.

Mechanical properties of the layers have a great influence on stress state in the initial and exploitation stages. Mechanical properties of hollow masonry units (1) (Fig. 1) and infill concrete (2) (Fig. 1), i.e. strength and deformational properties, are usually different. A few cases are possible: in the first case, the hollows can be filled with a material weaker than the masonry units ($E_{infil} < E_b$), e.g. concrete with polystyrene granule infill or other materials, which possess good thermal insulation qualities. In another case, hollows can be filled with concrete, which has greater strength than the strength of the masonry units ($E_{infil} > E_b$). This determines behaviour and mechanical properties, such as compressive strength and deformations, of the compressed masonry. If layer deformation properties are different, their strengths are used unequally. Depen-

ding on mechanical properties of layers, several behaviour cases are possible.

If layers have the same deformational properties ($E_{fil} = E_b$), they deform in the same way under compression and perform jointly until the moment of failure. In this case, strengths of layers are used to the maximum of their possibilities.

In other cases, the layers deform differently, depending on their deformational properties (modulus of elasticity). If greater stresses, which exceed elasticity limit of the layers, were involved, layer deformations would be different, i.e. $e_b > e_{infil}$ (where $E_b > E_{infil}$) or $e_b < e_{infil}$ (where $E_b < E_{infil}$), here e_b and e_{infil} – are longitudinal compressive deformations of masonry units and the infill concrete respectively. Layer strengths during failure are employed to a different extent, depending on their deformational properties.

1. Theoretical background for assessment of layer contact zone behaviour

Research shows (Bistrickaitė *et al.* 2004) that effective exploitation of composite construction layer material properties requires good bind between the layers, which ensures not only joint performance of the layers, but also distribution of stresses between them. If one of the layers is produced using the moulding method, the relation and bind between the components can be of two types: mechanical and physicochemical. Mechanical bind is achieved due to the presence of different pores, capillaries, roughness of the block surface and etc.; the group of physicochemical binds encompasses adsorption, which subsequently covers adhesion and cohesion. Thickness of layers influences adhesive strength. Size of internal stresses depends on layer thickness of contacting materials. The internal stresses appear due to deformation of different layers, under the influence of forces, humidity, temperature and etc. This is further proved by the diagrams in Fig. 2 – if shrinkage deformations are more equal in the contact zone, the deformation difference as well as shear stresses are reduced.

Conducted theoretical research (Marčiukaitis 1999, 2001) indicates that if masonry units and infill concrete shrink in a different way, different stresses, which can reduce strength of adherence in the contact zone, or even terminate it in some cases, are formed in the layers. Stresses produced due to shrinkage deformations are not big and practically do not exceed elasticity limit of the layer material.

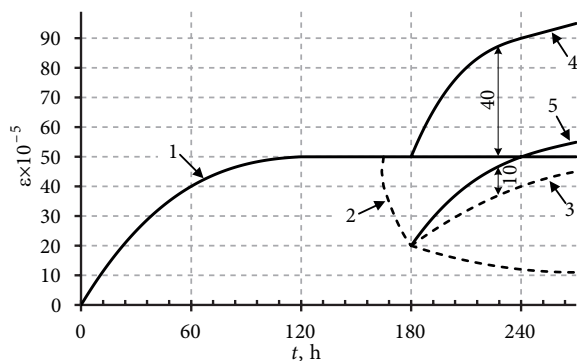


Fig. 2. Changes in concrete block and infill concrete shrinkage deformation development: 1 – blocks before use; 2 – block expansion due to external humidity; 3 – recursive deformations of the block along with infill concrete deformations; 4 – infill concrete deformations when the block is not humid; 5 – infill concrete deformations, which take place together with humid block deformations

Considering the fact that the contact zone of the layers is affected by continuity of deformations into account, the deformations in the contact zone are equal, i.e.:

$$\varepsilon_1(t) = \varepsilon_2(t). \quad (1)$$

Balance condition in the stress contact will be:

$$\varepsilon_1(t)E_1A_1 - [\varepsilon_2(t) - \varepsilon_1(t)]E_2A_2 = 0, \quad (2)$$

where: $\varepsilon_1(t)$, E_1 and A_1 are less shrinking layer shrinkage deformation, deformation module and cross-section area accordingly; $\varepsilon_2(t)$, E_2 and A_2 are more shrinking concrete shrinkage deformations, its deformation module and area accordingly.

Eq. (2) provides:

$$\varepsilon_1(t) = \varepsilon_2(t) \frac{E_2A_2}{E_1A_1 + E_2A_2}. \quad (3)$$

Less shrinking layer average stresses can be estimated from Eq. (3):

$$\sigma_1(t) = \varepsilon_2(t)E_1 \frac{E_2A_2}{E_1A_1 + E_2A_2}. \quad (4)$$

Average tensile stresses in a more shrinking layer will be:

$$\sigma_2(t) = \varepsilon_2(t)E_1 \frac{A_1}{A_2} \frac{E_2A_2}{E_1A_1 + E_2A_2}. \quad (5)$$

When the $\sigma_1(t)$ and $\sigma_2(t)$ stresses that form in layers, i.e. infill concrete and masonry units, are known, it enables estimating of shear (tangential) stresses in the layer contact:

$$\tau = \sigma_1(t) - \sigma_2(t). \quad (6)$$

If stress values of $\sigma_1(t)$ and $\sigma_2(t)$ (Eqs 3 and 4) are inserted into the formula (6) and some rearrangements are introduced, tangential stress value in the contact is acquired:

$$\tau = \varepsilon_2(t)E_1 \frac{E_2A_2}{E_1A_1 + E_2A_2} \left(1 - \frac{A_1}{A_2} \right). \quad (7)$$

If tangential stresses formed due to different layer shrinkage τ exceed shear strength of the contact τ_{\max} , layer adhesion is eliminated and shear strength is ensured by frictional force only, binds between the layers are of partial stiffness.

Otherwise, i.e. if the following condition is met:

$$\tau < \tau_{\max}. \quad (8)$$

Binds between layers can be considered stiff, layers performed jointly and their behaviour under compression is fundamentally based on deformational properties of the layers.

According to (Tschegg *et al.* 1995; Bistrickaitė *et al.* 2004) shear strength of contact can be estimated the following way:

$$\tau_{\max} = 0.35f_c^{0.195}, \quad (9)$$

where: f_c – concrete compressive strength of the weaker layer.

As indicated in Figure 2, in order to reduce tangential stresses in the contact it is necessary to meet certain technological requirements, i.e. before pouring infill concrete into the hollows, masonry units have to be humidified. Upon humidification, masonry units expand, also, when the hollows are filled with concrete, masonry units are additionally humidified by the free water present in the infill concrete. On the other hand, humid masonry units “take” water from infill concrete slower. Furthermore, the open surface, through which infill concrete evaporates water, is small. Therefore, the difference in shrinkage deformations of infill concrete and masonry units is lower and reduces stresses in contact.

2. Numerical modelling of stress strain state

While investigating behaviour and manner of masonry as a material failure, micro-modelling can be applied. Two approaches of micro modelling are applicable – simplified and detailed (Lourenço 1996). The conducted research (Lourenço 1996; Pina-Henrigues 2005; Haach 2009; Medeiros *et al.* 2013) shows that both methods produce reliable results. Micro modelling is often used when new masonry unit solutions are analysed (Jaafar *et al.* 2006; Thanoon *et al.* 2008; Porto *et al.* 2010; Del Coz Díaz *et al.* 2007; Ghiassi *et al.* 2013).

More accurate results are obtained when 3D model of the researched object is used. While investigating a set of masonry units with infill concrete hollows, provided masonry units are set in a “dry” way that is without filling bed joints with mortar, use of detailed micro-modelling can be advised. In such instances, every masonry unit is modelled as a separate body with its own geometry and material properties, and the contact zone between them is like a surface of a particular stiffness.

In many cases, mechanical characteristics of materials, which are used in production of masonry units, are established by testing appropriately sized samples extracted from the units (Marzahn 2003; Ganzerli *et al.* 2003; Badarloo *et al.* 2009). There is no

methodology to assess mortar properties of bed joints. Usually, generalised characteristics are applied (Zavalis, Jonaitis 2011), which are specified by performing specialised tests. While describing bed joints, contact zone with the masonry unit is modelled as binding surface, stiffness of which is presumed to be such that layer of masonry units and concrete would transfer compressive stresses appropriately.

The modelling task is even more complicated when masonry units are supported in a “dry” way, i.e. without mortar in bed joints. In such case, it is typical for a contact of masonry units in the bed joint to locally develop stress concentration due to roughness of the surface. In such case, it is advisable to use an appropriately stiff surface for modelling of the contact of masonry units in the bed joint. Stiffness of such surface can be described using stiffness of the bed joint. Stiffness of the bed joint k_n is described by the ratio of compressive stresses s_c and shear Dc (absolute deformations of the bed joint):

$$k_n = \sigma_c / \Delta c \text{ (N/mm}^3\text{)}. \quad (10)$$

Yet another critical issue is description of infill concrete and contact of a masonry unit. Shear stiffness of the contact depends on strength of adherence and stresses induced by shrinkage deformations of masonry units and infill concrete. Considering the above-mentioned facts, it can be deduced that since before the concrete is poured, when blocks are humidified, shrinkage deformations become close and tangential stresses, which damage adherence, are not formed due to shrinkage in the contact, also layers (walls) are bound by transverse edges, layers perform jointly and remain stiff when masonry fragment is compressed.

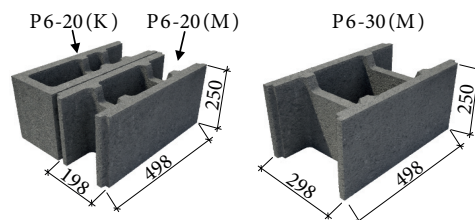


Fig. 3. Hollow concrete masonry blocks used in experimental program

3. Experimental program

Masonry samples set from concrete blocks with concrete filled hollows were built for compressed composite masonry stress state test. Samples were set from P6-20 (hollowness – 50%) and P6-30 (hollowness – 68%) hollow concrete blocks (Fig. 3).

Compressive strength of masonry units (concrete blocks) was established while testing it under brief static load in accordance with LST EN 772-1 (2011). Masonry unit and infill concrete properties are provided in Table 1.

While constructing the samples (masonry fragments), blocks were set in a “dry” way, i.e. without mortar in bed joints, and blocks were humidified, hollows were filled with concrete, this way, complex masonry samples were acquired.

In order to establish deformational properties of masonry units and stiffness of bed joints that have not been filled with concrete, samples made of the two masonry units were set in a “dry” way (Fig. 4).

Mechanical properties of masonry units and infill concrete were established by testing the blocks in accordance with LST EN 772-1 (2011), and control samples – cylinders of infill concrete in accordance with requirements of LST EN 12390-3.

Table 1. Masonry unit and infill concrete properties

Series	Code of specimens	Type of units	Compressive strength of units, N/mm ²		Mean modulus of elasticity of units concrete, E_{cm} , GPa	Infill concrete	
			Normalised f_b	Mean of units concrete		Mean cylinder compressive strength, N/mm ²	Mean modulus of elasticity E , GPa
P6-20	P6-20-1	P6-20(M)	10.53	28.23	2.92*	22.7	2.2
	P6-20-2		10.78				
	P6-20-3	P6-20(K)					
P6-30	P6-30-1	P6-30	6.78	29.49	3.2*	30.9	2.92
	P6-30-2						
	P6-30-3						

* determined from experimental tests (Fig. 4)

Mechanical properties of masonry unit blocks P–20 and P6–30 and the infill concrete are presented in Table 1.

Samples of hollow P6–20(30) blocks set in a “dry” way and masonry samples with filled hollows were tested by applying brief static compressive load. While testing the samples, the block, masonry and bed joint deformations were measured (Figs 4 and 5).

A model has been set for numerical analysis of compressive masonry sample P6-30, which was realised using DIANA software package. Numerical model has been developed by applying detailed micro modelling method, modelling exact masonry unit and infill concrete geometry with volumetric finite elements. A stiff steel beam, which transfers compressive load onto the fragment, is modelled applying the same principle. Upon evaluating symmetry, a ¼ fragment model is set (Fig. 6). The model is analysed using arch length method with Newton-Rapson Iteration considering that displacement and energy convergence conditions are equal to 10^{-3} .

Behaviour of masonry units and infill concrete is described applying the total strain crack model based on the fixed crack concept. Behaviour of tensile concrete is described by assessing tensile strength and tensile fracture energy of concrete by exponential dependence (TNO Diana 2005). Tensile strength of masonry units and infill concrete is calculated in accordance with tension and compressive strength dependences provided in LST EN 1992-1-1 (EC2). Tensile fracture energy of concrete G_f is estimated in accordance with CEP FIP recommendations (CEP 1990):

$$G_f = G_{F0} \left(f_c / f_{cm0} \right)^{0,7}, \quad (11)$$

where: G_{F0} – the base value of fracture energy; f_c – compressive strength, f_{cm0} – constant considered to be equal to 10 N/mm^2 .

Behaviour of compressed concrete is described by parabolic dependence provided in DIANA software package, taking into consideration compressive strength of concrete established while testing control samples and estimated fracture energy of compressed concrete G_{Fc} (Sandoval *et al.* 2012):

$$G_{Fc} = 15 + 0,43f_c - 0,0036f_c^2, \quad (12)$$

Contact between masonry units (concrete blocks) is modelled using plane elements as a surface capable of transferring only compressive stresses. Contact between infill concrete and masonry units is considered to be stiff. Contact zone of bed joints of blocks that was not filled with mortar (dry) is described using compressive (normal) and shear stiffness.

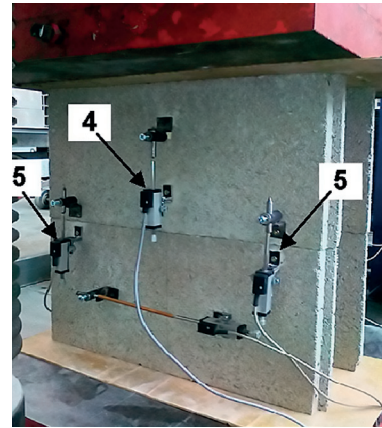


Fig. 4. Sample of a hollow block set in a “dry” manner, scheme of testing and measuring tool deployment

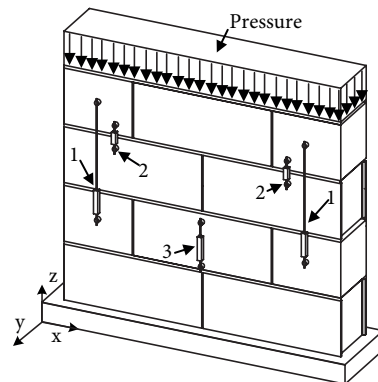


Fig. 5. Experimental scheme of masonry with filled hollows and tool deployment

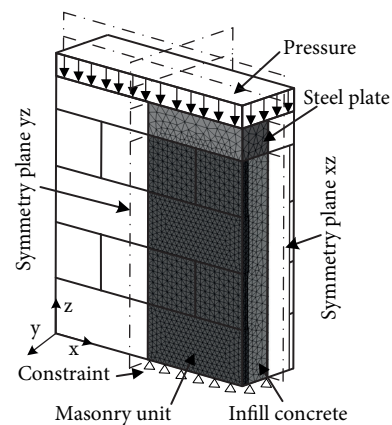


Fig. 6. Numerical masonry fragment model

Stiffness of the contact of masonry units (bed joint) was estimated performing special experiments, i.e. samples consisting of two grouted blocks set in a “dry” way was tested applying brief static compressive load (Fig. 4). During the experiment, block and contact deformations were measured, and block material

compressive strength and elasticity modulus and contact stiffness were estimated. Compressive stiffness of bed joint contact zone was estimated using Eq. (10) from the results of the experiment, shear stiffness of contact k_τ was estimated in accordance with dependence:

$$k_\tau = \frac{k_n}{2(1+\nu)}, \tag{13}$$

where: k_n – normal (compressive) bed joint stiffness, ν – Poisson’s ratio.

Parameters of numerical model are presented in Table 2.

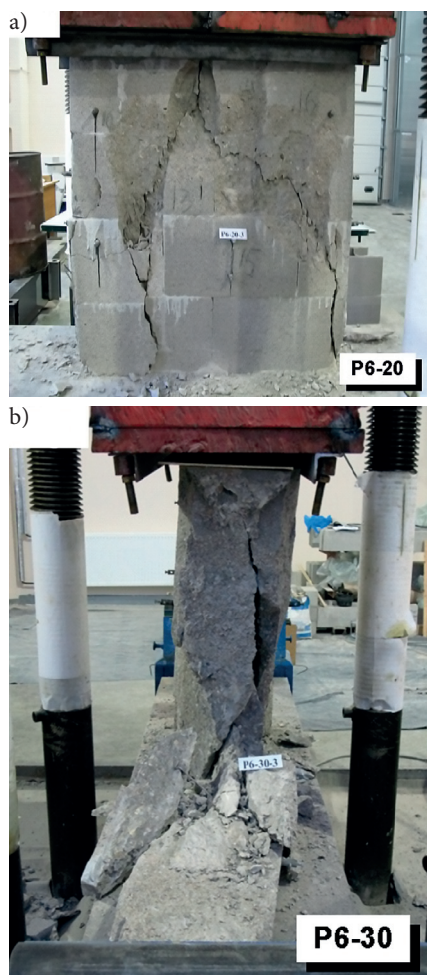


Fig. 7. Failure of P6-20 (a) and P6-30 (b) concrete blocks with concrete infill specimen of masonry

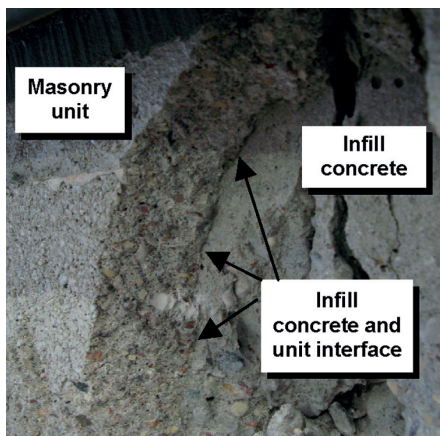


Fig. 8. Contact zone of a masonry unit and concrete infill

Table 2. Material properties of the numerical model

Parameter	Units	Infill concrete	Masonry unit
Compressive strength, f_c	N/mm ²	25.27	24.55
Tensile strength, f_{ct}	N/mm ²	3.09	2.9
Tensile fracture energy, G_F	Nmm/mm ²	0.069	0.053
Compressive fracture energy, G_{Fc}	Nmm/mm ²	25.27	24.55
Poisson’s ratio, ν	-	0.2	0.22
Normal stiffness of the joint, k_t	N/mm ³	44.5	
Shear stiffness of the joint, k_τ	N/mm ³	18.2	

Table 3. Experimental results

Series	Code of specimens	Compressive strength of masonry, N/mm ²		Modulus of masonry elasticity, E, GPa	
		Specimens	Mean	Specimens	Mean
P6-20	P6-20-1	21.5	22.9	26.0	25.2
	P6-20-2	23.3		23.6	
	P6-20-3	23.9		25.9	
P6-30	P6-30-1	27.4	26.5	30.7	28.8
	P6-30-2	24.5		24.7	
	P6-30-3	27.5		31.2	

3. Experiment results and its analysis

Experiment and numerical modelling results of P6-20(30) hollow blocks with concrete filled hollows masonry samples are presented in Table 3 and Figs 7–11.

Character of the failure of masonry samples is similar to that of the concrete prism failure (Fig. 7). Cracks were formed under the load of 90–100% of failure load, i.e. before the failure of the sample, sudden (crumbling) failure took place. Until the moment of failure, blocks and infill concrete performed mutually, no layer scaling was observed (Fig. 8).

Longitudinal (vertical) sample deformations before stresses 50–60% of compressive strength are similar to longitudinal deformations of control samples (cylinder) (Fig. 9). Longitudinal deformations of masonry sample blocks and bed joints revealed suffi-

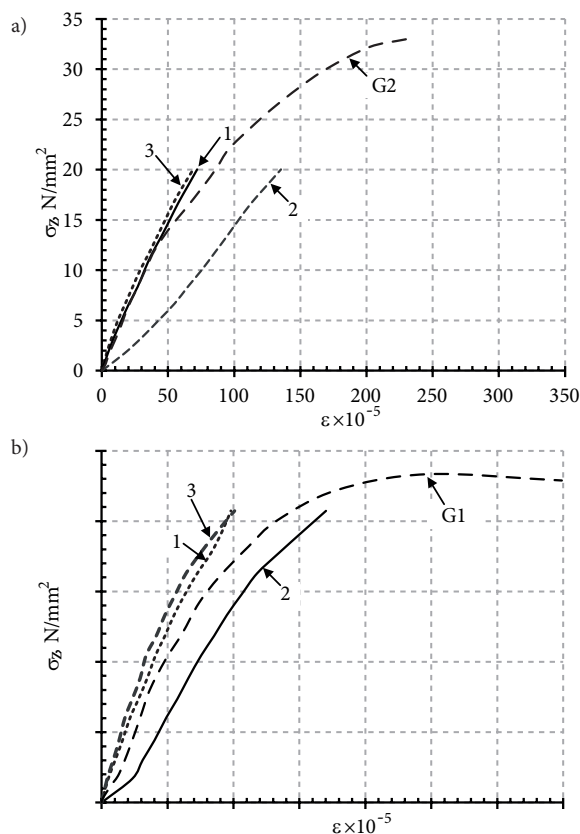


Fig. 9. Deformations of masonry set with concrete infill (a) P6-20 and (b) P6-30 blocks: 1 – longitudinal deformation of a specimen; 2 – longitudinal deformation of the bed joint, 3 – longitudinal deformation of a block; G1 and G2 – longitudinal deformation of the infill concrete control sample

ciently good joint performance of the blocks and infill concrete.

Distribution of compressive stresses obtained by numerical modelling is presented in Figs 10 and 11.

Numerical modelling results of compressed masonry revealed that compressive stresses in both, grouted blocks and infill concrete are distributed unevenly. This is determined by different elasticity modulus of hollow block concrete and infill concrete ($E_b < E_{infil}$), also, contact stiffness of the bed joint is significantly smaller than stiffness of concrete blocks. A significant increase of compressive stresses can be observed in the bed joint zone of infill concrete (Fig. 10). Compressive stresses are also distributed unevenly in the blocks (Figs 10a and 11). Web assumes greater compressive stresses than shells (Fig. 11a). Distribution of stresses in infill concrete and hollow block indicates that both elements mentioned above are involved in joint performance; stresses are distributed depending on deformational properties of infill concrete and hollow block concrete. Diagrams of numerical modelling and σ_c - ϵ_c obtained during the experiments are presented in Fig. 11.

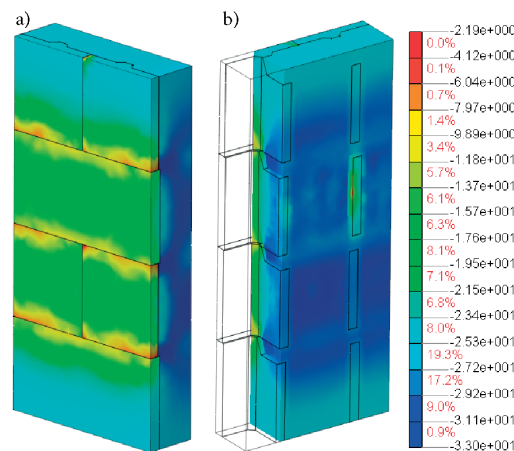


Fig. 10. Distribution of P-30 masonry fragments compressive stresses

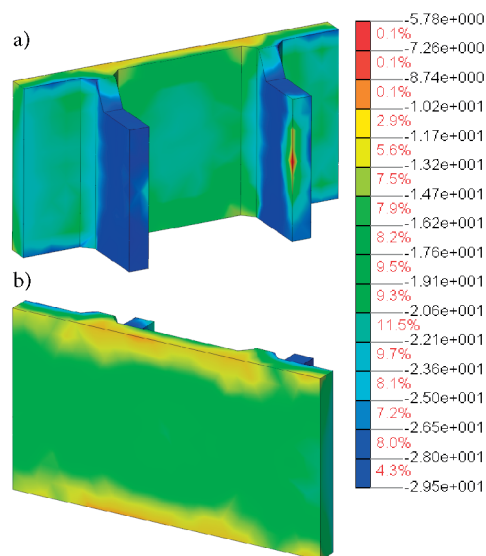


Fig. 11. Distribution of compressive stresses of concrete blocks within the P6-30 masonry fragment

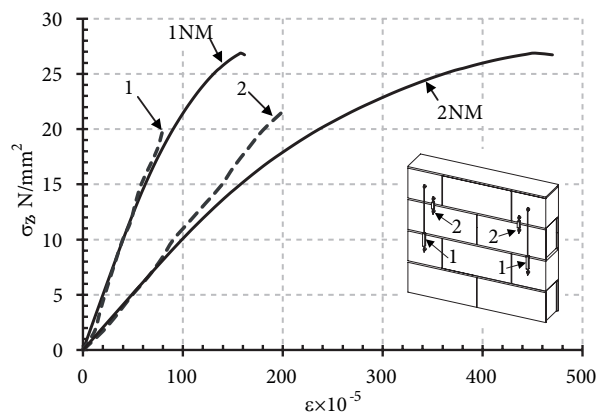


Fig. 12. Diagram of σ_c stresses and ϵ_c relative deformations: 1 and 1NM – of the masonry estimated by experiments and numerical modelling respectively; 2 and 2NM – of the bed joint zone estimated by experiments and numerical modelling respectively

Stress and relative deformation values estimated by numerical modelling were assumed during the experiments in the deformation measuring zones. As shown in Fig. 12, σ_c - ε_c dependences in the masonry and the bed joint zones estimated applying numerical modelling match fine with the ones estimated during the experiments. Masonry samples modulus of elasticity that was calculated (numerical modelling $E_{cal} = 25$ GPa) and determined during the experiments ($E_{obs} = 28.8$ GPa) differs in up to 15%. Estimated and experimental average compressive strength of P6-30 masonry fragment is equal to $f_{cal} = 26.72$ N/mm² and $f_{obs} = 26.5$ N/mm², accordingly. The performed analysis revealed that detailed micro modelling of masonry stress deformations produces rather accurate results.

Conclusions

Experimental and numerical stress state research of hollow blocks with infill concrete proved the assumption that the difference between shrinkage deformations of grouted blocks and infill concrete is reduced by humidifying masonry units. The difference of shrinkage deformations of infill concrete and block does not damage the contact, and reliable joint performance of infill concrete and blocks is ensured until the very moment of compressed masonry failure. In such case, stiff bind of layers can be used while modelling.

Detailed numerical micro-model of the compressed masonry provides sufficiently accurate computing results. σ_c - ε_c dependences in masonry and bed joint zones acquired through the means of numerical modelling correspond to those estimated during the experiments. Modulus of elasticity of masonry samples was estimated by calculations (numerical modelling $E_{cal} = 25$ GPa) and experiments ($E_{obs} = 28.8$ GPa) differs up to 15%. Estimated and experimental average compressive strength of a masonry samples is equal respectively to $f_{cal} = 26.72$ N/mm² and $f_{obs} = 26.5$ N/mm². Detailed numerical micro modelling can be applied while conducting research of compressed masonry stress strain analysis.

References

Badarloo, B.; Tasnimi, A. A.; Mohammadi, M. S. 2009. Failure criteria of unreinforced grouted brick masonry based on a biaxial compression test, *Scientia Iranica Transaction A: Civil Engineering* 16(6): 502–511.

Bistrickaitė, R.; Marčiukaitis, G.; Žilinskas, R. 2004. *Precast and cast in-situ concrete slabs with residual mould*. Kaunas: Technologija. 229 p. (in Lithuanian).

Comité Euro-International Du Béton (CEB). 1990. *CEB-FIP model code for concrete structures*. Lausanne, Switzerland.

Del Coz Díaz, J. J.; García Nieto, P. J.; Betegón Biempica, C.; Prendes Gero, M. B. 2007. Analysis and optimization of the heat-insulating light concrete hollow brick walls design by the finite element method, *Applied Thermal Engineering* 27(8–9): 1445–1456.
<http://dx.doi.org/10.1016/j.applthermaleng.2006.10.010>

Fonseca, F.; S.; Siggard, K. 2012. Replacement of portland cement with supplemental cementitious materials in masonry grout, in *Proceedings of the 15th International Brick and Block Masonry Conference*, 2012, Florianopolis, Brazil.

Ganzerli, S.; Rosslow, J.; Young, T.; Kres, K.; Mujumdar, V. 2003. Compression strength testing for nonstandard concrete masonry units, in *Proceedings of The 9th North American Masonry Conference*, 2003, Clemson, South Carolina, USA, 60–71.

Ghiassi, B.; Oliveira, D. V.; Lourenço, P. B.; Marcari, G. 2013. Numerical study of the role of mortar joints in the bond behavior of FRP-strengthened masonry, *Composites Part B: Engineering* 46: 21–30.
<http://dx.doi.org/10.1016/j.compositesb.2012.10.017>

Haach, V. 2009. *Development of a design method for reinforced masonry subjected to in-plane loading based on experimental and numerical analysis*: PhD thesis summary. University of Minho.

Jaafar, M. S.; Alwathaf, A. H.; Thanoon, W. A.; Noorzaei, J.; Abdulkadir, M. R. 2006. Behaviour of interlocking mortarless block masonry, *Construction Materials* 159(August): 111–117. <http://dx.doi.org/10.1680/coma.2006.159.3.111>

LST EN 1992-1-1. 2007. *Eurokodas 2. Gelžbetoninių konstrukcijų projektavimas. 1–1 dalis. Bendrosios ir pastatų taisyklės*.

LST EN 772-1. 2011. *Mūro gaminių bandymo metodai. 1 dalis. Gniuždymo stiprio nustatymas*.

LST EN 12390-3. 2003. *Betono bandymas. 3 dalis. Bandinių stipris gniuždant* (in Lithuanian).

Lourenço, P. B. 1996. *Computational strategies for masonry structures*: PhD thesis summary. Delft University of Technology.

Marčiukaitis, G. 1999. Estimation of redistribution of stresses between layers of composite masonry walls, in *Proceedings of The 6th International conference "Modern Building Materials, Structures and Techniques"*, 19–22 May 1999, Vilnius: Technika, 104–109 (in Lithuanian).

Marčiukaitis, G. 2001. Shrinkage influence on stress-strain state of composite masonry members, *Civil Engineering* 7(3): 177–183 (in Lithuanian).

Marzahn, G. 2003. Extended investigation of mechanical properties of masonry units, in *Proceedings of the 9th North American Masonry Conference*, 2003, Clemson, South Carolina, USA, 813–824.

Medeiros, P.; Vasconcelos, G.; Lourenço, P. B.; Gouveia, J. 2013. Numerical modelling of non-confined and confined masonry walls, *Construction and Building Materials* 41: 968–976.
<http://dx.doi.org/10.1016/j.conbuildmat.2012.07.013>

Oan, A. F.; Shrive, N. 2012. Effect of construction method on shear resistance of concrete masonry walls, in *Proceedings of the 15th International Brick and Block Masonry Conference*, 2012, Florianopolis, Brazil.

- Pina-Henriques, J. 2005. *Masonry under compression: failure analysis and long-term effects*: PhD thesis summary. University of Minho.
- Porto, F.; Mosele, F.; Modena, C. 2010. Compressive behaviour of a new reinforced masonry system, *Materials and Structures* 44(3): 565–581. <http://dx.doi.org/10.1617/s11527-010-9649-x>
- Sandoval, C.; Roca, P. 2012. Study of the influence of different parameters on the buckling behaviour of masonry walls, *Construction and Building Materials* 35: 888–899. <http://dx.doi.org/10.1016/j.conbuildmat.2012.04.053>
- Thanoon, W. A.; Alwathaf, A. H.; Noorzaeei, J.; Jaafar, M. S.; Abdulkadir, M. R. 2008. Nonlinear finite element analysis of grouted and ungrouted hollow interlocking mortarless block masonry system, *Engineering Structures* 30(6): 1560–1572. <http://dx.doi.org/10.1016/j.engstruct.2007.10.014>
- TNO Diana 2005. *DIANA finite element analysis*. The Netherlands.
- Tschegg, E. K.; Rotter, H. H.; Bourgund, H.; Jussel, P. 1995. Fracture mechanical behaviour of aggregate cement matrix interfaces, *Journal of Materials in Civil Engineering* 7(4): 199–203. [http://dx.doi.org/10.1061/\(ASCE\)0899-1561\(1995\)7:4\(199\)](http://dx.doi.org/10.1061/(ASCE)0899-1561(1995)7:4(199))
- Zavalis, R.; Jonaitis, B. 2011. The analysis of stress deformation state peculiarities of masonry units and bed joints, *Engineering Structures and Technologies* 3(3): 105–111 (in Lithuanian). <http://dx.doi.org/10.3846/skt.2011.12>

BLOKŲ SU BETONU UŽPILDYTOMIS TUŠTYMĖMIS GNIUŽDOMOJO MŪRO ĮTEMPIŲ BŪVIO SKAITINĖ IR EKSPERIMENTINĖ ANALIZĖ

R. Zavalis, B. Jonaitis, G. Marčiukaitis

Santrauka. Straipsnyje pateikiama betoninių blokų su betonu užpildytomis tuštymėmis gniuždomojo mūro įtempių būvio analizė. Mechaninėms tokio mūro savybėms įtakos turi pradiniai įtempiai, kuriuos sukelia skirtingos užpildymo betonu ir mūro gaminių traukiosios deformacijos. Užpildymo betonu ir betoninių blokų elgsena analizuojama taikant tikslų skaitinį mikromodeliavimą. Eksperimentais nustatyta, kad blokų su užpildytomis betonu tuštymėmis mūro deformacijos artimos užpildymo betonu deformacijoms. Skaitiniu modeliavimu gautos σ - ε priklausomybės ir gniuždomasis mūro stipris gerai sutampa su eksperimentais nustatytais reikšmėmis.

Reikšminiai žodžiai: tuštymėtumas, betono mūro gaminiai, užpildymo betonas, traukumas, skaitinis modeliavimas.

Robertas ZAVALIS. PhD student at the Department of Reinforced Concrete and Masonry Structures, Vilnius Gediminas Technical University (VGTU). Research interests: masonry and masonry structures.

Bronius JONAITIS. Dr, Associate Professor at the Department of Reinforced Concrete and Masonry Structures, Vilnius Gediminas Technical University (VGTU). Research interests: theory of reinforced concrete behaviour, masonry and masonry structures, strengthening of structures.

Gediminas MARČIUKAITIS. Dr Habil, Professor at the Department of Reinforced Concrete Structures, Vilnius Gediminas Technical University (VGTU). Research interests: mechanics of reinforced concrete, masonry and layered structures, new composite materials, investigation and renovation of buildings.